

2007

# Integrated Broadband MicroPhotonics Beamformer for Adaptive Nulling in Smart Antennas

Budi Juswardy  
*Edith Cowan University*

Kamal Alameh  
*Edith Cowan University*

Yong Lee

---

[10.1117/12.696371](https://doi.org/10.1117/12.696371)

This article was originally published as: Juswardy, B., Alameh, K. , & Lee, Y. (2007). Integrated Broadband MicroPhotonics Beamformer for Adaptive Nulling in Smart Antennas. Proceedings of SPIE, Smart Materials, Nano-and Micro-Smart Systems. Perth, Australia. SPIE. Original article available [here](#)

Copyright 2008 Society of Photo-Optical Instrumentation Engineers (SPIE). One print or electronic copy may be made for personal use only. Systematic reproduction and distribution, duplication of any material in this paper for a fee or for commercial purposes, or modification of the content of the paper are prohibited.

This Conference Proceeding is posted at Research Online.

<http://ro.ecu.edu.au/ecuworks/4950>

# Integrated Broadband MicroPhotonic Beamformer for Adaptive Nulling in Smart Antennas

Budi Juswardy<sup>\*1</sup>, Kamal Alameh<sup>1</sup>, and Yong Tak Lee<sup>2</sup>

<sup>1</sup>Centre for MicroPhotonic Systems, Edith Cowan University, Joondalup, WA6027, AUSTRALIA.

<sup>2</sup>Department of Information and Communications, Gwangju Institute of Science and Technology, Gwangju, KOREA.

## ABSTRACT

This paper presents an integrated MicroPhotonic beamformer that processes RF-modulated optical signals to adaptively synthesise multiple broadband nulls in smart phased-array antennas. The beamformer is designed to operate at centre frequency of 5.6 GHz with 1 GHz bandwidth. Designs of the different photonic and RF components are presented. Simulation results show that a 4-element MicroPhotonic broadband smart antenna beamformer operating in the 5.1-6.1-GHz range can generate three broadband nulls, with less than 1.121° beam squint.

**Keywords:** Adaptive nulling, broadband beamforming, phased-array antennas, true-time-delay generation, RF photonics.

## 1. INTRODUCTION

The enormous growth of the number of broadband wireless subscribers has driven the need for increasing the capacity of wireless networks to accommodate larger volumes of broadband subscribers. Smart antennas could be employed to achieve higher spectrum use and network capacity, and also more efficient use of transmitted energy. The directivity of a smart antenna can be adjusted to maximise the wanted signals and minimise the interfering signals. This allows for higher signal-to-noise ratio, lower transmission power, and permits greater frequency reuse and greater bandwidth within the same cell [1]. Therefore, smart-antenna-based efficient multimedia and rich high-content data communication systems can find applications in many markets such as automobiles, aircrafts, ships, transport vehicles and other military or consumer-electronic products.

In general, a smart antenna, which generates arbitrary radiation patterns, consists of multiple antenna array elements in conjunction with appropriate signal processing. To obtain an optimal radiation pattern for broadband transmission, the signals received by or transmitted from the antenna array must be accurately *time-compensated* with respect to the wavefront, and this delay equalization must be frequency independent.

Most of the current research on smart antenna has been focused on broadband beam steering. But less has been given to the important ability of a phased array system to place broadband nulls at chosen angular coordinates to minimise the interference signal [2]. The *null steering* problem is fundamentally different from *broadband beam steering*. In current broadband beamformer, although the *main lobe* of the array pattern is fixed in a specified spatial direction over a wide frequency range, the *null locations* are not fixed in their spatial location, but, dependent on the frequency. Broadband null steering requires a beamformer that can generate variable, rather than fixed, true time-delays. Electronic phase-shifting circuits that are currently used to achieve time-delay are frequency dependent; and conventional RF signal processing techniques are limited by the loss of metallic media. Digital Signal Processing (DSP) is currently thwarted by limited resolution and bandwidth of analog-to-digital converter [3]. This problem can be solved by developing new time-shifting devices based on very accurate true time-delay circuits (which are frequency independent).

Recent advances in microelectronics and fiber optic telecommunications have made low-cost and high-quality microelectronics and photonics components available [4], [5]. This opens an opportunity to merge electronics and optics for RF processing to improve the performance of smart antennas. Therefore, a "MicroPhotonic" based smart antenna integrating microelectronics and photonics can have attractive features such miniaturization, broadband, and multi-functional RF processing capability. Such an antenna system can have all the RF front-end signal processing such as

\* [bjusward@student.ecu.edu.au](mailto:bjusward@student.ecu.edu.au), telp: +61 431-7439-36, [comps.ecu.edu.au](http://comps.ecu.edu.au)

For a 4-element antenna, with main lobe at  $\theta$  and nulls located along angular coordinates,  $\theta_1$ ,  $\theta_2$ , and  $\theta_3$ , the array factor takes the form

$$AF_4(\theta) = \sum_{m=0}^{N-1} W_m e^{jmkd \sin(\theta)} = \left( e^{jkd \sin(\theta)} - e^{jkd \sin(\theta_1)} \right) \left( e^{jkd \sin(\theta)} - e^{jkd \sin(\theta_2)} \right) \left( e^{jkd \sin(\theta)} - e^{jkd \sin(\theta_3)} \right) \quad (2)$$

By expanding Eq. (2), we obtain

$$AF_4(\theta) = x^3 - x^2 \left( e^{j\omega\tau_{21}} + e^{j\omega\tau_{22}} + e^{j\omega\tau_{23}} \right) + x \left( e^{j\omega\tau_{11}} + e^{j\omega\tau_{12}} + e^{j\omega\tau_{13}} \right) - e^{j\omega\tau_{01}} \quad (3)$$

In which there is 7 time-delay terms can be observed, where  $x = \exp(jkd \sin(\theta))$ , and

$$\begin{aligned} \tau_{21} &= \frac{d}{c} \sin(\theta_1), \tau_{22} = \frac{d}{c} \sin(\theta_2), \tau_{23} = \frac{d}{c} \sin(\theta_3) \\ \tau_{11} &= \frac{d}{c} [\sin(\theta_1) + \sin(\theta_2)], \tau_{12} = \frac{d}{c} [\sin(\theta_1) + \sin(\theta_3)], \tau_{13} = \frac{d}{c} [\sin(\theta_2) + \sin(\theta_3)] \\ \tau_{01} &= \frac{d}{c} [\sin(\theta_1) + \sin(\theta_2) + \sin(\theta_3)] \end{aligned} \quad (4)$$

These  $2^4-1=7$  delays could be selected from  $8 \times n$  delays generated by the optical cavities. The gain of an amplifier integrated to a photoreceiver element can independently be adjusted to equalize the amplitude of the delayed RF signal detected by that photoreceiver.

Figure 2 illustrates the concept of weight synthesis for a broadband smart antenna element. The low-noise amplifier (LNA) pre-amplifies the input RF received by the antenna element, to boost the modulation efficiency of the VCSEL array. The RF splitter equally splits the input RF into  $K_N$  RF signals, which are transmitted via RF channels to modulate the  $K_N$  elements of the  $1 \times K_N$  VCSEL array integrated on the VCSEL/photoreceiver chip. The Diffractive Optical Elements (DOEs) collimate and route the Gaussian beams generated by the VCSEL array. Each RF-modulated collimated optical beam generated by a VCSEL element propagates within the optical substrate and undergoes several reflections in a cavity whose width defined by the DOEs. Every time a beam hits the DOEs, a small fraction of the power of that beam is transmitted through the DOEs for detection and amplification by an element of the wideband photoreceiver array that is integrated on the VCSEL/ photoreceiver chip, while the remaining large fraction is reflected and routed to for subsequent delayed photodetection. The photoreceiver can be adjusted to either produce a delayed RF signal or zero signal. An RF combiner adds (or subtracts) the amplified RF photocurrents to generate the output RF signal that is equivalent to the multiplication of the input RF signal by a weight, which is the sum of many delayed versions of the RF signal.

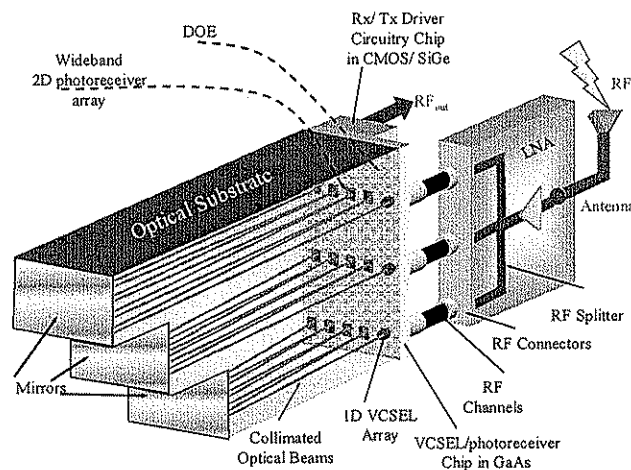


Figure 2: Concept of weight generation for a broadband smart antenna receiver for one antenna element [3].

Figure 4 shows the interface between the VCSEL/ photoreceiver chip and the optical substrate, and also illustrates the propagation of the optical beams inside the optical substrate. The VCSEL element generates laser beam of modulated RF signal. The glass layer is used over the VCSEL/ photoreceiver chip for protection. The DOE plate is inserted between the VCSEL/ photoreceiver chip and the optical substrate. The DOE comprises two sections. The first section is the VCSEL collimator, which is a hologram capable of collimating and steering VCSEL beam, while the second section (dashed) acts as a lens relay that prevents the cavity beam from diverging as it propagates, and also maintains its diameter within an adequate range. The DOE can be appropriately coated to provide any desired reflectivity. As the cavity beam hits the DOE, a large portion of its power is reflected inside the optical cavity while a small fraction of its power is transmitted through the DOE and the glass layer and then detected by one of the photoreceivers. For a cavity length  $L$  and a photoreceiver spacing  $d$ , the steering angle  $\theta$  of the VCSEL collimator is  $\arctan(d/2L)$ , and the incremental delay time between successive photoreceivers is

$$\Delta\tau = \frac{2n_o\sqrt{L^2 + (d/2)^2}}{c} \quad (5)$$

where  $n_o$  is the refractive index of the optical substrate, and  $c$  is the speed of light in vacuum. The gain of each photoreceiver is independently reconfigured to compensate for the RF and optical losses by using limiting amplifier. Also, a negative gain can be synthesized by having two post-amplification amplifiers, one inverting and another one is non-inverting RF amplifier.

### 3. INTEGRATED MICROPHOTONIC BROADBAND NULL BEAMFORMER IMPLEMENTATION

The main building blocks for smart antenna receivers are LNAs, VCSEL drivers, VCSEL arrays, true-time delay, photodiode arrays, transimpedance amplifier, gain control components, signal adder/ combiner, and adaptive control system. The choice of the technology used to fabricate the device is dependent on several factors. Reducing the cost of electro-optical system is one of the main goals of most joint-research efforts [7]. Another goal is to build a robust & reliable system. The focus is to design a low-cost, high-speed, Integrated, low-power System [8], [9]. Low cost IC paradigm normally consists of reducing fabrication costs, improving the yield and increasing the volume [7]. CMOS process offers an attractive technology as a choice of device fabrication, as it is the mainstream of most of the integrated circuits used in consumer products. The process is quite mature, therefore the yield is good and the cost is comparatively low compared to other process like Bipolar process, SiGe, and GaAs. Therefore, the design of most of the building blocks in this integrated MicroPhotonic smart antenna would be based on the CMOS technology. Some of the important building blocks are discussed in the following sections.

#### 3.1 Low Noise Amplifier (LNA) Design

The requirements for the LNA for the integrated MicroPhotonic smart antenna is that it should operate at 5.6 GHz, be capable of amplifying signals over a broad bandwidth (1GHz) with low noise figure. To raise the gain, and also to have a high signal-to-noise ratio (SNR) for further signal processing, the LNA should be designed to have single-to-differential conversion.

A suitable candidate for the LNA is the new topology wideband LNA proposed in [10]. Conventional wideband amplifiers are having either distributed or resistive feedback topology. The distributed approach often suffers from high power consumption and low gain, and the method to obtain gain by using inductive peaking is usually suitable only for narrowband applications. The noise figure of typical resistive feedback amplifiers is usually not low enough. To raise the wideband gain, the proposed LNA (Figure 5) must include a single-to-differential conversion, consisting of common gate (M1/ M2) and common source (M4) amplifiers in parallel. The common gate amplifier consists of NMOS (M1) and PMOS (M2) transistors stacked in series, which carry the bias current between the supplies. Therefore, the noise contributions from both transistors M1 and M2 are cancelled. With this differential output sensing topology, the load resistor noise is also less significant.

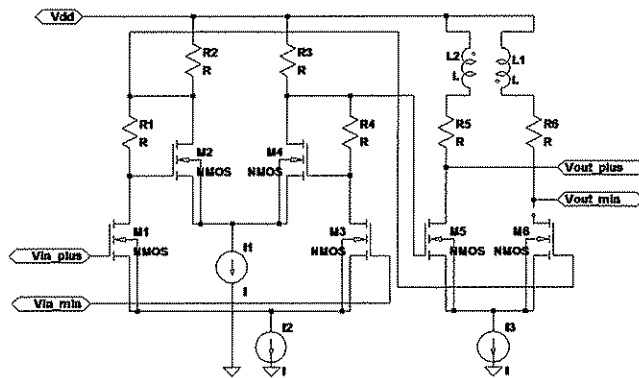


Figure 7: Circuit diagram of the preamplifier used in VCSEL driver of Fig. 6 [12].

### 3.3 True Time-delay generation

True time-delay generation is required to generate broadband nulls, as previously described in Section 2. For broadband signal processing, the time delay generation must be independent of frequency, capable of providing time delay over a broad frequency range. Phased shift circuits normally have limited operational bandwidth. Photonic structures can realise frequency independent true-time delays. The proposed true-time delay generator in this paper is based on the reflection of several collimated optical beams in micro cavities as previously explained in Section 2. Other photonic true-time delay generation methods having compact and practical hardware include the fibre ring resonator [13], programmable integrated optical spiral planar lightguide (Little Optics) [14], and the Fiber Bragg gratings [15] in the optical cavity substrate to add the delay time.

### 3.4 Transimpedance and Limiting amplifier

After the true-time delay generation inside the optical cavity, the light has to be converted back to the electrical domain. The photodiode transforms the light intensity to a proportional current, which is then amplified and converted to voltage for further signal processing. This current-to-voltage conversion is performed by transimpedance amplifier. There are some design requirements for amplifier, such as transimpedance value, signal, noise, supply rejection, output swing [11], input sensitivity, overload response, stability, bandwidth, output impedance (S22), non-linearity, and jitter [16].

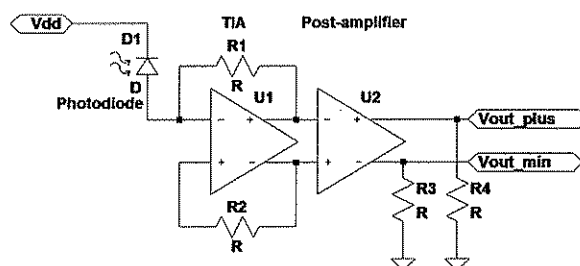


Figure 8: Block diagram of photodiode amplifier

Figure 8 shows the block diagram of the photodiode amplifier. It consists of two stages, one stage is the transimpedance stage, and the second one is the post amplifier stage. The amplifier topology selected is the differential amplifier, because it is suitable for the CMOS implementation, especially when using a low-level input signal under low-supply voltage in submicron CMOS [17]. Single-ended topology is not suitable because it is very susceptible to supply noise and plagued by stability problems stemming from parasitic feedback paths, despite the advantages of high-gain, high-bandwidth, and low-power consumption. When there are other high-speed circuits present on the same substrate, large

### 3.5 RF Combiner

RF signal combiners are required to combine the output RF signals from the photodiode amplifiers. Low loss, compact size, system compatibility and good isolation between signal branches are the requirements for RF combiners [18]. There are several RF signal combining techniques, such as Resistive Adders, Wilkinson Combiners and Active RF Signal Adders. Resistive adders isolate different branches by attenuating each input signal with an isolation equals to twice the value of the insertion loss for each path. A resistive adder is a broadband topology, but its power loss is quite high. Wilkinson combiners provide a relatively low loss, but it is very sensitive of the lengths of the interconnections between different antenna paths, and creates routing issues if many RF signals are combined.

On the other hand, active RF combining has the ability to add gain to the output. Figure 11 illustrates an active RF combiner designed for the MicroPhotonic smart antenna beamformer shown in Fig. 3. This circuit has the capability of controlling the bias current to adjust the gain for weight generation needed for beamsteering. The control signal comes from an adaptive/control system. By tuning the voltage of the bias terminals, the amplitude of each RF signal from every photodiode amplifier can be adjusted so that any non-uniformity of the signal strength from different photodiodes can be compensated for, and the signals to be combined for beamsteering can be selected.

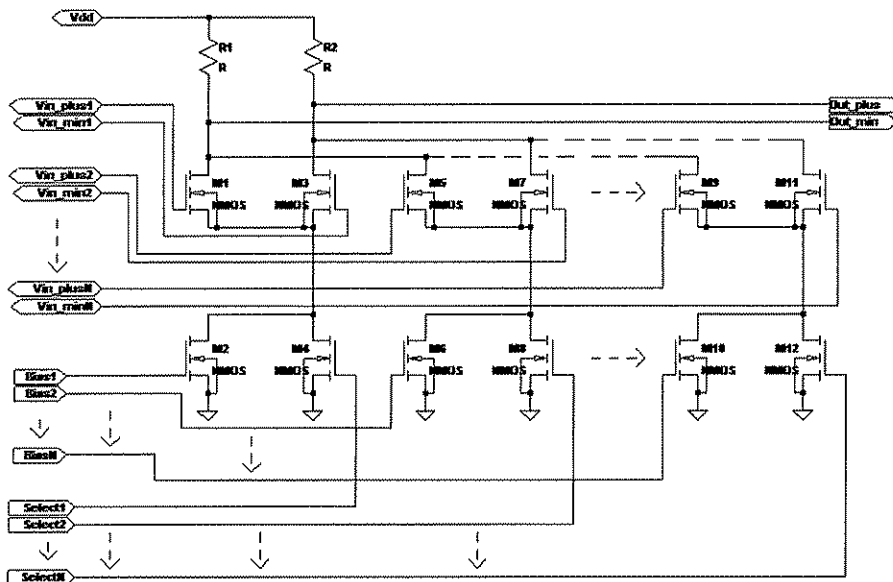


Figure 11: Schematic for the active RF signal combiner

### 3.6 Control System for Weight Generation

To generate the weight needed for beamsteering, a "control system" is needed to select the delays generated from the antenna arrays. The control system should have a specific algorithm that maximises the Signal-to-Interference Ratio (SIR), thus minimising the weight variance and Mean Square Error (MSE). The implementation of the algorithm can be performed electronically through a simple analog or digital signal processor. Digital signal processing algorithm can be divided into two main categories: the fixed and adaptive algorithm [1]. Maximum Signal-to-Interference Ratio, Minimum Mean-Square Error, Maximum Likelihood (ML), and Minimum Variance algorithms belong to fixed algorithm. Examples of Adaptive beamforming algorithms are Least Mean Square (MLS), Sample Matrix Inversion (SMI), Recursive Least Square (RLS), Conjugate Gradient Method (CGM), Constant Modulus (CM) and combinations of these algorithms. Each of these algorithms has advantages and disadvantages that need to be considered when selecting the suitable algorithm.

Figure 13 shows the directional and gain fluctuation of the main beam at different frequency. It is seen that, for an operation frequency of 5.6 GHz, the direction of the main beam is slightly off from the target of  $5^\circ$  by  $0.749^\circ$ . For a 4-element smart antenna operating at mid frequency of 5.6 GHz, the gain of the main beam changes by less than 3 % over 1-GHz bandwidth, and less than  $1.121^\circ$  beam squint. Figure 14 shows the field pattern polar plot of the main lobe, the side lobe and the nulls for 4-element antenna at 5.6GHz.

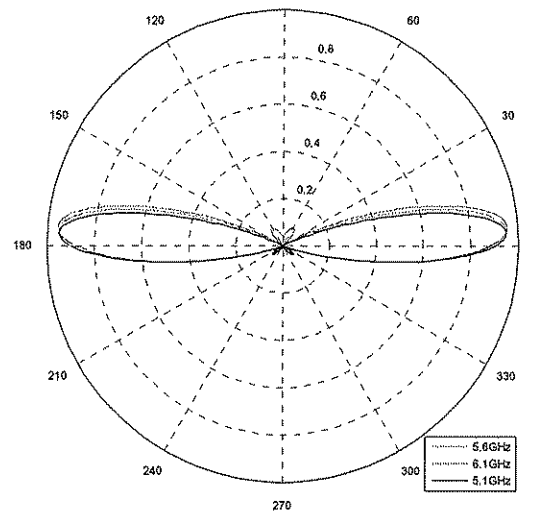


Fig 14: The polar plot of 4-element MicroPhotonic Smart Antenna Array Factor

## 5. CONCLUSION

The structure and design of a MicroPhotonic smart antenna beamformer has been described, which uses a VCSEL array, photoreceiver array, and micro-optics integrated on an optical substrate to synthesise broadband spatial nulls. Simulation results have shown that a 4-element MicroPhotonic broadband smart antenna beamformer operating in the 5.6-GHz band might generate 3 nulls independent of the operating frequency within 1GHz bandwidth, with slight degradation in main beam gain, and less than  $1.121^\circ$  beam squint. The MicroPhotonic beamformer can be realised with a  $1 \times 8$  VCSEL array, a  $8 \times 64$  photoreceiver array and a diffractive optical element integrated on an optical substrate.

## REFERENCES

1. Frank Gross, "Smart Antennas for Wireless Communications", McGraw-Hill, 2005
2. Zmuda, H., E. N. Toughlian, M. A. Jones, and P.M. Payson, "Photonic architecture for Broadband Adaptive Nulling with Linear and Conformal Phased Array Antenna." Fibre and Integrated Optics 19: pp137-154, 2000
3. Kamal E. Alameh, Kamran Eshraghian, Selam Ahderom, Mehrdad Raisi, Mike Myung-Ok Lee, Rainer Michalzik, "Integrated MicroPhotonic Broadband Smart Antenna Beamformer," DELTA, p. 208, Second IEEE International Workshop on Electronic Design, Test and Applications, 2004
4. Mike Salib et al., "Silicon Photonics", Optical Technology & Applications, Intel Technology Journal Vol 8, No 2, Corporate Technology Group, INTEL Corp., 2004
5. Peter Kirckpatrick et al., "10 Gb/s Optical Transceiver: Fundamentals and Emerging Technology", Optical Technology & Applications, Intel Technology Journal Vol 8, No 2, Intel Communications Group, INTEL Corp., 2004